Analytical Methods

ROYAL SOCIETY OF CHEMISTRY

PAPER

View Article Online
View Journal | View Issue

Cite this: *Anal. Methods*, 2022, **14**, 2100

Small molecules released from islets of Langerhans determined by liquid chromatography – mass spectrometry†

Emmanuel O. Ogunkunle, Matthew J. Donohue, Daniel J. Steyer, Damilola I. Adeoye, Wesley J. Eaton and Michael G. Roper *

Islets of Langerhans are the endocrine tissue within the pancreas that secrete hormones for maintenance of blood glucose homeostasis. A variety of small molecules including classical neurotransmitters are also released from islets. While the roles of most of these small molecules are unknown, some have been hypothesized to play a critical role in islet physiology. To better understand their role on islet function, a liquid chromatography-tandem mass spectrometry (LC-MS/MS) method was developed to separate and quantify 39 small molecules released from islets. Benzoyl chloride derivatization of analyte molecules was used to impart retention and facilitate electrospray ionization efficiency. Separation was achieved on a 2.1 × 150 mm column packed with 2.7 μm core–shell C_{18} particles. Calibration curves showed excellent linearity between the concentration and analyte response, with relative standard deviations of the analyte responses below 15% and limits of detection from 0.01–40 nM. The method was applied to examine small molecules released from murine and human islets of Langerhans after static incubation and perfusion with glucose. Results showed a decrease in secretion rates with increasing glucose concentration for most of the analytes. Secretion rates were found to be higher in human islets compared to their murine counterpart. This method will be useful in understanding the roles of small molecules in biological systems.

Received 8th March 2022
Accepted 15th April 2022

DOI: 10.1039/d2ay00402j

rsc.li/methods

1. Introduction

Diabetes mellitus is a metabolic disease resulting from an inability to maintain blood glucose homeostasis.[1] The International Diabetes Federation (IDF) estimated that 1 in 10 adults aged 20–79 (537 million) had diabetes mellitus in 2021, with the number projected to reach 643 million by 2030, and 783 million by 2045.[2] Over 90% of the population affected by diabetes has type 2 diabetes mellitus (T2DM),[3,4] which is characterized by an inability to secrete enough insulin to regulate the effect of high glucose, or due to a lack of response to the secreted insulin.[1] Unfortunately, there is no known cure for diabetes, making it a global health challenge.

The process of blood glucose regulation is impacted largely from the release of hormones, such as insulin and glucagon, from islets of Langerhans. Insulin is released from β-cells in response to high blood glucose and initiates glucose uptake by peripheral tissues and the inhibition of hepatic glucose output; glucagon is released from α-cells during low glucose conditions initiating glycogenolysis and gluconeogenesis.[5–7] In addition to these hormones, a variety of small molecules are also released from islets and thought to directly or indirectly affect hormone secretion, and ultimately glucose regulation.[8–11] Although the effects of some of these molecules have been investigated, the role for the majority are unknown and the delineation of their actions would be helped by analytical methods that can quantify the numerous analytes that are released from islets.

Micellar electrokinetic chromatography with laser-induced fluorescence (MEKC-LIF) detection has been used for separation and detection of primary amines released from islets of Langerhans.[12–14] The release of D-amino acids were also investigated using a chiral MEKC-LIF method by the addition of sodium deoxy cholate to the buffer system.[14] In these methods, the migration time reproducibility was <5% and the LOD for most compounds were less than 10 nM. While the methods were robust, when they were used with samples from murine[12–14] and human[13] islets, the numerous peaks observed made it difficult to identify based only on migration time.

Liquid chromatography-tandem mass spectrometry (LC-MS/MS) is an alternative method well suited for the analysis of a wide range of small molecules.[15] LC-MS/MS provides better confidence in analyte identification, especially when operated in multiple reaction monitoring (MRM) mode since each analyte has a unique transition.[16] Due to the polar nature of most small molecules, they have little or no retention on commonly

Department of Chemistry and Biochemistry, Florida State University, 95 Chieftain Way, Tallahassee, FL 32306, USA. E-mail: mroper@fsu.edu; Tel: +1-850-644-1846

† Electronic supplementary information (ESI) available. See https://doi.org/10.1039/d2ay00402j

used reversed phase LC (RPLC) columns. This lack of retention not only leads to poor resolution but also short retention times where analytes can elute with salts present in the sample, thereby suppressing electrospray ionization (ESI) efficiency.[17] One approach to increase retention is to derivatize analytes with a hydrophobic tag.[18] While multiple tags have been developed,[19] benzoyl chloride (BzCl) reacts quickly with 1° and 2° amines as well as alcohols under mild reaction conditions, produces stable derivatives, is inexpensive, and has a commercially available ^{13}C analog that can be used to label internal standards (IS) for improved quantification by MS/MS.[20–23]

Various reports have been published using BzCl derivatization with LC-MS/MS for the determination of small molecules, including neurochemicals and metabolites, from various biological samples.[20–23] For example, a report was published targeting 17 neurochemicals released from intact rat brains using microdialysis sampling.[21] The method was further optimized to improve sensitivity and reproducibility, after which it was used to determine 70 small molecules from various biological samples.[23] However, there has been no report of the method to investigate islet secretions. Furthermore, while sub 2 μm LC particles have been used for high efficiency separations of benzoylated analytes,[21,23] the use of core–shell particles for these separations[24–27] allow many of the benefits of the small particles to be realized without the necessity of high pressure systems.[28]

In this report, we optimized a LC-MS/MS method using a column packed with 2.7 μm core–shell C_{18} particles for quantitation of 39 targeted small molecules released from islets of Langerhans. Limits of detection (LOD) ranged from 0.01 to 40 nM for the analytes. Using the method, small molecules released from murine and human islets were quantified after incubation in low and high glucose levels. Furthermore, dynamic changes in the secretion of the small molecules were monitored using a PDMS/glass hybrid microfluidic device fabricated to house, perfuse, and collect fractions from both murine and human islet secretions.

2. Materials and methods

2.1 Chemicals and reagents

Sodium hydroxide (NaOH) was purchased from EMD Millipore (San Diego, CA). Dextrose and tricine were from Fisher Scientific (Pittsburgh, PA). LC grade acetonitrile (ACN) was from VWR (Radnor, PA). d4-Acetylcholine (d4-ACh) was from CDN Isotopes Inc. (Pointe-Claire, QC). All solutions were made with HPLC grade submicron filtered water (Fisher Chemical, Fair Lawn, NJ). Stock solutions of serine (Ser), threonine (Thr), asparagine (Asn), glutamine (Gln), alanine (Ala), histidine (His), aspartate (Asp), tyrosine (Tyr), γ-aminobutyric acid (GABA), valine (Val), methionine (Met), leucine (Leu), phenylalanine (Phe), tryptophan (Trp), arginine (Arg), taurine (Tau), glycine (Gly), glutamate (Glu), dopamine (DA), serotonin (5-HT), proline (Pro), *trans*-4-hydroxy proline (Hyp), cysteine (Cys), lysine (Lys), isoleucine (Ile), α-aminobutyric acid (α-ABA), β-aminobutyric acid (β-ABA), β-homoserine (β-HSer), tyramine (TryA), citrulline (Cit), kynurenine (Kyn), 2-aminoadipic acid (Aad), ornithine (Orn), histamine (Hist), 5-hydroxytryptophan (5-HTP), *N*-acetylcysteine (NAC), epinephrine (Epi), and acetylcholine (ACh) were made in LC water and diluted to working concentrations using a balanced salt solution (BSS) containing 25 mM tricine, 125 mM NaCl, 5.9 mM KCl, 1.2 mM $MgCl_2$, 2.4 mM $CaCl_2$, and various glucose concentrations as described in the text, and the pH was adjusted to 7.4 with NaOH.

2.2 Benzoyl chloride derivatization

For production of calibration curves, 100 μL of a standard mixture of small molecules (concentrations given in Section 3.3) in BSS was mixed with 50 μL of 100 mM sodium carbonate (pH 9.2) and 50 μL 2% BzCl (by volume in ACN). The mixture was vortexed and allowed to react for 30 s before quenching with 50 μL of IS (composition described below). The ratio of sample : carbonate buffer : BzCl : IS was always 2 : 1 : 1 : 1 (v/v/v/v). IS were produced by derivatization of the small molecules with ^{13}C benzoyl chloride using the method described above. Because ACh did not derivatize, d4-ACh was spiked into the IS solution to a final concentration of 100 nM. To obtain desalted components for building the MRM method described in Section 2.3, analytes and IS were extracted with dichloromethane (DCM), followed by evaporation with N_2 gas and reconstitution in 20% ACN containing 0.1% formic acid (FA).

2.3 LC-MS instrumentation

LC-MS experiments were performed using a Thermo Scientific (Waltham, MA) Vanquish Flex UHPLC system with a Split Sampler Module and a Thermo Scientific TSQ Quantis triple quadrupole mass spectrometer. 10 mM ammonium formate with 0.1% FA was used as mobile phase A (MPA) and ACN containing 0.1% FA used as mobile phase B (MPB). Separations were performed on a 2.1 × 150 mm, 2.7 μm, 160 Å pore ES-C_{18} column (Halo Peptide, Mac-Mod Analytical, Chadds Ford, PA) used with a 2.1 × 5 mm, 2.7 μm, 160 Å pore ES-C_{18} guard column (Mac-Mod Analytical). The injection volume was 5 μL and the mobile phase flow rate was 0.25 mL min^{-1}. The column temperature was held constant at 25 °C in still air mode while the autosampler was set to 4 °C.

The TSQ Quantis mass spectrometer was operated in MRM mode. Electrospray settings were: spray voltage of 3500 V, sheath gas at 4.19 L min^{-1}, auxiliary gas of 6.4 L min^{-1}, sweep gas 1.5 L min^{-1}, ion transfer tube temperature of 300 °C, and a capillary temperature of 275 °C. For MS/MS optimization, desalted sample was directly infused into the mass spectrometer at a flow rate of 50 μL min^{-1}. The most intense and consistent fragments were used for building the MS/MS method for each analyte and IS. During LC-MS/MS runs, a time managed MRM was performed where the MRM transition for specific analytes were examined in a retention time (RT) window, defined as the RT ± 0.50 min (Table S-1†). A dwell time of 50 ms was used for each transition.

2.4 Isolation and culture of islets of Langerhans

All animal experiments were performed under guidelines approved by the Florida State University Animal Care and Use Committee, protocol 202000078. Murine islets were obtained by

digesting the pancreas from two male CD-1 mice (20–40 g) with collagenase as previously described.[29,30] The islets from both mice were combined and incubated at 37 °C with 5% CO_2 in RPMI 1640 (Corning, Manassas, VA) containing 11 mM glucose, L-glutamine, 10% fetal bovine serum, 100 U mL^{-1} penicillin, 100 μg mL^{-1} streptomycin, and 10 μg mL^{-1} gentamycin. Islets were used the day after isolation.

Human islets were purchased from Prodo Laboratories (Aliso Viejo, CA) from donors with no history of diabetes. The islets were recovered according to the protocol established by Prodo Laboratories, followed by incubation in Prodo Islet Media Standard PIM(S) at 37 °C and 5% CO_2 for at least 1 day. Human islet samples were from deidentified cadaveric organ donors and therefore exempt from Institutional Review Board approval. Islets from two donors were used in separate experiments and donor characteristics are shown in Table S-2.† Islets from Donor 1 were used in a static incubation experiment while islets from Donor 2 were used in a perfusion experiment.

2.5 Static incubation of islets

For static incubation experiments, 20 human or murine islets were removed from culture media and rinsed three times with prewarmed BSS containing 1 or 3 mM glucose, respectively. The rinsed islets were then placed in a 250 μL microcentrifuge tube containing 100 μL of the same BSS solution and incubated at 37 °C with 5% CO_2. After one hour, 90 μL of the supernatant was removed and replaced with 90 μL BSS containing 22.2 mM glucose for human islets and 22 mM glucose for murine islets to bring the final glucose concentration to 20 mM. The islets were then incubated for 1 h at 37 °C with 5% CO_2, after which another 90 μL of the supernatant was removed. Supernatant from both incubations were derivatized separately as described in Section 2.2.

2.6 Dynamic perfusion of islets

The microfluidic device fabrication, setup, and characterization are similar to that described elsewhere[31] and given in more detail in the ESI.† Prior to each use of the microfluidic device, the system was conditioned by flowing RPMI media with serum for 30 min and stopping the flow for 30 min. This procedure was followed by 30 min of perfusion with BSS containing 1 or 3 mM glucose for human or murine islets, respectively. 25 islets were held in a dish containing 1 or 3 mM prewarmed glucose in BSS for 10 min in the incubator. The islets were then loaded into the islet chamber and allowed to settle to the bottom. The islet chamber was sealed with PCR film, placed in the incubator for 10 min, after which the input and output tubing were connected. BSS with 1 or 3 mM glucose was delivered to the islets at 5 μL min^{-1} for 30 min prior to fraction collection. Islets were perfused with low glucose (1 or 3 mM) for 10 min, followed by high glucose (20 mM) for 30 min, and low glucose (1 or 3 mM) for another 10 min. The fractions were collected in a 96-well plate, derivatized, and injected into the LC-MS.

2.7 Data analysis

Chromatograms were analyzed using Xcalibur (Thermo Scientific) software. The software was used to integrate the peak area that coincided with the retention time window for each analyte and IS. Calibration curves were constructed by plotting the ratio of the average blank-subtracted analyte : IS peak area for 3 injections against the concentration of analyte injected. Error bars in all plots are equal to ±1 standard deviation (SD) unless otherwise noted. Linear least-squares were used to fit the data and the resulting regression equations were used to calculate the unknown concentrations of analytes from islet samples. LOD for each analyte were calculated using 3 times the SD of the blank peak area divided by the slope of each calibration curve. Comparison of sample means was performed using a paired two-tailed *t*-test, unless otherwise noted, with significance determined when $p < 0.05$. Resolution (R_s) between peaks was calculated using the difference in retention times and the average of the peak widths at baseline.

3. Results and discussion

To investigate the role of small molecules in islet physiology, an analytical method capable of determining numerous classes of low abundance small molecules is required. Derivatization with BzCl and analysis with LC-MS/MS has previously been used for the determination of small molecules in other biological samples,[20–23] but it has not been applied to islet secretions. BzCl reacts significantly faster under mild conditions than other derivatizing agents commonly used for increasing hydrophobicity of polar analytes.[32] In addition, it is inexpensive and a commercially available isotopically labelled analog can be used for improved quantitation. By combining the advantages of this reagent with separation using a core–shell RPLC column, we set out to quantify up to 39 small molecules released from murine and human islets of Langerhans in static and dynamic perfusion conditions in response to changing glucose levels.

3.1 MS optimization

Our initial effort focused on identifying the precursor and product ions for each analyte through direct infusion. Upon reaction with BzCl, all analytes showed benzoylation (except for ACh), yielding single-, double-, and triple-labelled species as detected by a precursor ion scan. All benzoylated analytes yielded protonated products $[M + H]^+$ by positive ESI while for ACh, the molecular ion, M^+, was observed. Other adducts such as $[M + Na]^+$ and $[M + NH_4]^+$ were also detected but the signal was either low or not reproducible compared to the $[M + H]^+$ ions.

The most abundant product ion for most benzoylated analytes was the benzoyl fragment (*m*/*z* 105). For such analytes, the MRM transition from the product ion to the benzoyl fragment (105) was selected for monitoring. However, for some compounds such as 5-HT, Kyn, Hist, and Orn, unique product ions with similar or higher relative abundance compared to the benzoyl fragment were selected for monitoring. The transitions for IS were found to be similar to those of the analytes with a mass shift of M + 4 for d4-ACh and M + 6 for ^{13}C-labelled

benzoylated analytes. As observed with the analytes, the most dominant product ion was the ^{13}C-benzoyl fragment (m/z 111), except for 5-HT, Kyn, and Orn where unique product ions were used. The optimized MRM parameters for the analytes and IS are shown in Table S-1.†

3.2 LC optimization

To resolve the benzoylated species in a reasonable time, a C_{18} column 2.1 × 150 mm (i.d. × length) using 2.7 μm core–shell particles (2.7 μm total diameter, 1.7 μm solid core) was used. These columns achieve high efficiency separations while maintaining a low back pressure.[28] A scouting gradient was used to determine the retention behavior of the analytes. Initial gradient conditions with less than 5% MPB led to distorted peak shapes for early eluting species such as His, Tau, Ser, and Asn; therefore, 5% MPB was the starting condition for optimizing gradients, flow rates, and column temperatures. A shallow gradient led to peak broadening, with the most pronounced found for Hyp and Pro. With the shallow gradient (5–100% B over 20 min), peak widths of 0.79 and 0.75 min were observed with these analytes, respectively. A steep gradient (5–100% B over 10 min) reduced these to 0.20 and 0.35 min, but at the expense of R_s. Therefore, a compromise between R_s and peak width was found with a non-linear gradient: 0–0.2 min, 5–10% B; 0.2–7.1 min, 10–25% B; 7.1–8.1 min, 25–30% B; 8.1–12 min, 30–100% B; 12–15 min, 100% B; 15–25 min, 5% B (equilibration). This gradient produced peak widths of 0.21 and 0.44 min for Hyp and Pro, respectively. Calculated R_s for some critical pairs at the shallow, steep, and optimized (non-linear) gradients are shown in Table S-3.† The flow rate was set to 0.25 mL min^{-1} to stay below the pressure limit of the column (600 bar). With these conditions, the backpressure ranged from 145–440 bar during the separation.

With the optimized conditions, the 39 analytes were separated and detected in 13 min (Fig. 1). Time managed MRM was used to perform a particular MRM transition within a retention time window. This procedure reduced the number of MRM transitions that were monitored, allowing collection of more data points for each peak. Combined, the optimized procedures led to highly reproducible separations with retention times less than 1% RSD (n = 5 injections). Without the time managed MRM or a 10 min equilibration time, less reproducible results were observed.

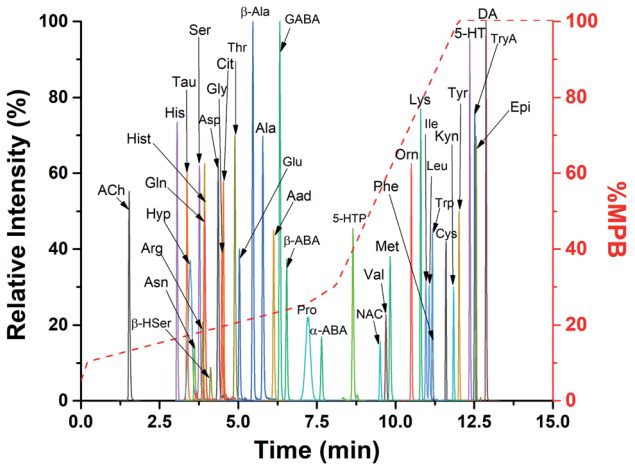

Fig. 1 Reconstructed ion chromatograms of 39 analytes. Extracted ion chromatograms for each analyte at 1000 nM (100 nM for ACh) were normalized to the highest intensity and overlaid. The optimized % MPB is shown as the red dashed line and corresponds to the right y-axis.

3.3 Analytical performance

To assess the analytical performance of the developed method, calibration curves were constructed for all analytes in the high salt solution that would be found when working with islets. Standards were made with 3 mM glucose in BSS using concentrations ranging from 2.5 to 1250 nM for Tyr, GABA, Val, Met, Leu, Phe, Trp, Arg, Glu, DA, 5-HT, Pro, Hyp, Cys, Lys, Ile, β-Ala, Kyn, Orn, Hist, Epi, and ACh, with their respective IS at a concentration of 100 nM. A higher concentration range was used for Ser, Thr, Asn, Gln, Ala, His, Asp, Tau, Gly, α-ABA, β-ABA, β-HSer, Cit, Aad, 5-HTP, and NAC, from 12.5 to 12 500 nM with their IS concentrations at 1000 nM. For all analytes, high linearity over the concentration ranges were obtained with $R^2 > 0.99$ (Table 1). Calculated LODs ranged from 0.01 to 40 nM and the RSD of analyte/IS peak area ratios were <15% across all concentrations examined (n = 3 injections). Carryover was <5% as determined by sequential injections of a 500 nM standard analyte mixture and a blank injection (n = 5). These values are comparable to other methods that have used BzCl derivatization.[21–23] Upon completion of method development, levels of these small molecules released from murine and human islet of Langerhans were quantified upon glucose stimulation.

3.4 Analysis of secretions from murine and human islets

To quantify the small molecules released from islets of Langerhans, static incubations of murine and human islets were performed. Islets from these species differ in architecture and cellular composition, but the effects of these differences on islet function are still being investigated. In the first experiment, murine islets were incubated in BSS with 3 or 20 mM glucose for 1 h and the supernatant was derivatized. In the second experiment, human islets were incubated in BSS with 1 or 20 mM glucose for 1 h and the supernatant was derivatized in a similar manner.

The quantified amounts released from both islet species at low (black bars) and high (white bars) glucose concentrations are shown in Fig. 2. With murine islets (Figure 2A), 30/39 targeted small molecules were detected, while 27/39 were detected from human islets (Fig. 2B). Of the 27 detected from human islets, only Hist was unique to the human samples. β-ABA, Cit, DA, and TryA were exclusively detected in murine islets. The concentrations of all small molecules decreased with increasing glucose concentration from the murine islets, which is similar to that observed elsewhere.[12–14] There was a significant difference (p < 0.05, n = 3) between all secretions at 3 and 20 mM glucose. The measured values at the different glucose levels after normalizing to the incubation volume and numbers of

Table 1 Figures of merit for benzoylated analytes

Analyte	LOD (nM)	Sensitivity (nM^{-1})	R^2	RSD (%)	Analyte	LOD (nM)	Sensitivity (nM^{-1})	R^2	RSD (%)
ACh	0.1	0.0071	0.9999	6	Pro	0.05	0.0047	0.9999	4
His	0.6	0.0005	0.9996	3	α-ABA	5	0.0007	0.9998	10
Tau	0.4	0.0005	0.9997	3	5-HTP	0.1	0.0006	0.9991	3
Hyp	6	0.0004	0.9999	3	NAC	4	0.0004	0.9997	4
Asn	0.9	0.0007	0.9981	11	Val	0.8	0.0068	0.9989	5
Ser	7	0.0004	0.9994	9	Met	0.5	0.0055	0.9988	8
Arg	0.1	0.0063	0.9992	7	Orn	0.1	0.0124	0.9994	5
Gln	0.7	0.0007	0.9994	7	Lys	0.1	0.0801	0.9999	4
Hist	0.01	0.0173	0.9990	4	Ile	3	0.0064	0.9991	7
β-HSer	2	0.0010	1.0000	3	Phe	0.4	0.0100	0.9989	8
Asp	20	0.0004	0.9971	10	Leu	3	0.0068	0.9998	10
Gly	40	0.0006	0.9972	10	Trp	0.3	0.0061	0.9993	7
Cit	0.7	0.0008	0.9994	4	Cys	0.4	0.0020	0.9999	7
Thr	4	0.0008	0.9993	6	Kyn	0.1	0.0081	0.9995	3
Glu	2	0.0065	0.9992	7	Tyr	3	0.0062	0.9980	13
β-Ala	0.3	0.0071	0.9999	4	5-HT	0.1	0.0040	1.0000	7
Ala	8	0.0008	0.9999	4	TryA	0.1	0.0043	0.9999	6
Aad	10	0.0008	0.9999	8	Epi	0.2	0.0116	0.9999	7
GABA	0.1	0.0080	1.0000	4	DA	0.5	0.0077	0.9998	4
β-ABA	2	0.0007	0.9998	4					

islets, are in close agreement with our previous report that used MEKC[12] (Table S-4†). A similar trend of decreasing concentration of small molecules at high glucose concentration was also observed from the human islets, except for β-Ala and Kyn which increased with high glucose incubation. The average concentration of Hist detected was independent of the glucose challenge. Of the 27 small molecules detected, there was a significant difference ($p < 0.05$, $n = 3$) in the secretions at 1 and 20 mM glucose for all analytes except Tau, Asn, β-Ala, and Ala. It should be noted that these experiments were conducted using multiple islets obtained from 2–4 mice, ensuring a relatively averaged view of release from murine islets. However, islets from only one human donor were examined. Therefore, while the changes between glucose levels were quantified for this donor, how the levels may differ between other donors was not examined.

3.5 Perfusion experiment

Microfluidic devices are ideal for monitoring profiles of cellular secretions due to a high level of control over the localized cellular environment, ease of automation, and the ability to perform experiments with little dilution.[33,34] To monitor the dynamic secretion profiles from islets, a microfluidic device was used to house and perfuse a group of murine or human islets with varying glucose levels. A PDMS/glass hybrid microfluidic device with two inlets for glucose, an islet chamber, and an outlet to collect fractions was used. The details of the device and its fabrication are given in the ESI.† Prior to running islet experiments, the response and delay time of the system was evaluated by alternating the perfusion of fluorescein and BSS through the device at 5 μL min^{-1}. BSS was flowed through the device for 10 min, followed by a step change to 500 nM fluorescein for another 10 min. This process was alternated for 50 min with perfusate collected every 2 min into a 96-well plate. The fluorescence in each well was read with a plate reader and the response time of the device, defined as the time required to increase or decrease the signal from 10% to 90%, was 2 fractions or 4 min (Fig. S-1†).

After device characterization, 25 murine islets were loaded into the device and perfused with 3 mM glucose for 30 min. Islets were then perfused with 3 mM glucose for 10 min, followed by 20 mM glucose for 30 min, and switched back to 3 mM glucose for 10 min, with fractions collected every 2 min. The fractions were then derivatized and injected into the LC-MS system. Two separate experiments were performed using islets from different mice. In experiment 1, at 3 mM glucose, 25/39 targeted small molecules were detected and quantified with secretion rates ranging from 7 to 450 fmol per islet per min. Fig. 3 shows the secretion rates of small molecules released from murine islets as a function of time. The secretion rates of Gly, Asp, Ala, Leu, and Val were found to be higher than others. Secretion rates of small molecules in experiment 2 were relatively lower compared to experiment 1. As shown in Fig. S-2,† secretion rates ranged from 10 to 430 fmol per islet per min with Asp, Gly, and Leu having higher secretion rates than others. Both experiments exhibited a similar pattern of release of gradually decreasing secretion rates with increasing glucose concentration, before returning to prestimulatory levels as the glucose level was lowered.

For human islets experiments, 25 human islets from Donor 2 were loaded into the device and perfused with 1 and 20 mM glucose in a pattern similar as described for murine islets. Two experiments were performed using islets from the same donor. For the first experiment, 26/39 small molecules were detected with secretion rates ranging from 3 to 540 fmol per islet per min, with secretion rates for Ala, Gly, Pro and Lys higher than others Fig. 4. In experiment two, secretions ranged from 3

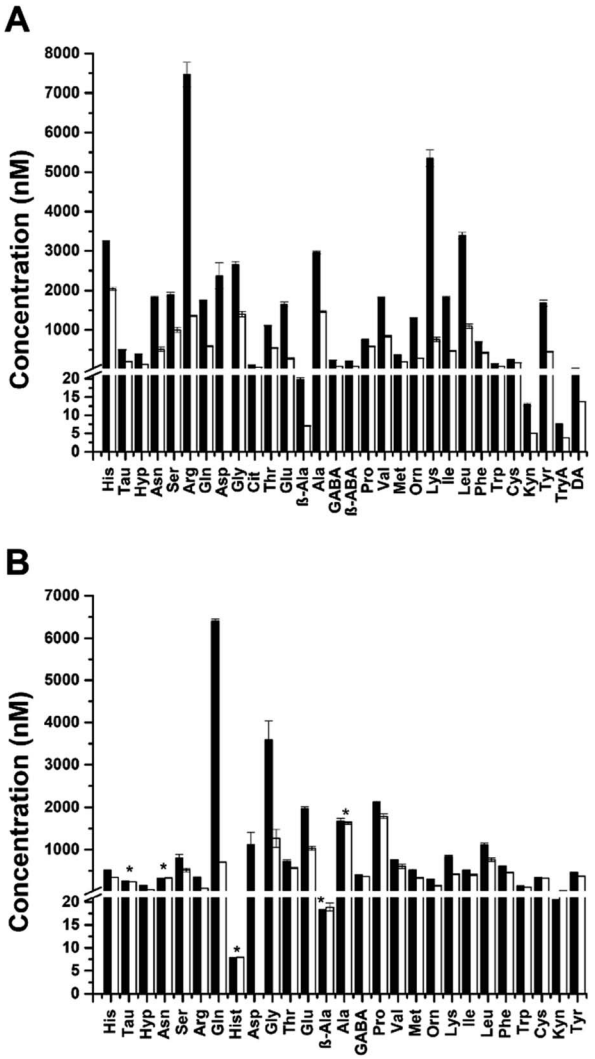

Fig. 2 Static incubations of islets. Both plots show the levels of small molecules released from 20 islets. (A) Murine islets were stimulated with 3 (black bars) and 20 (white bars) mM glucose and their levels measured by the optimized method. (B) Small molecules released from human islets stimulated with 1 (black) and 20 (white) mM glucose were quantified. For all conditions, derivatized samples were injected three times and a paired two-tailed *t*-test was used to compare sample means. All levels of small molecules were found to be significantly different from low to high glucose, except those noted by * ($p > 0.05$).

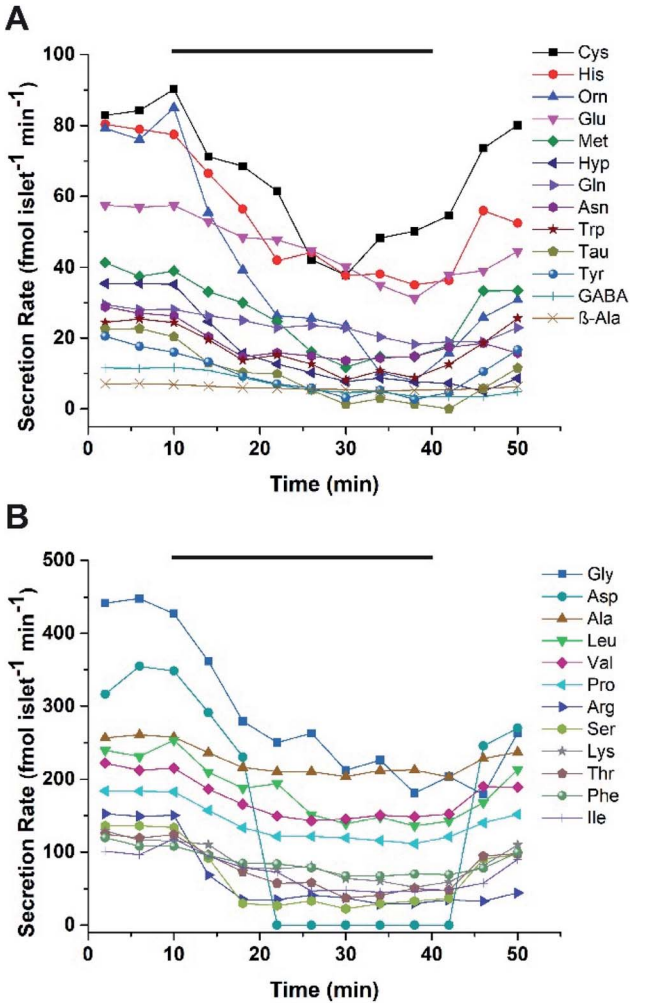

Fig. 3 Release profiles from murine islets. Secretions from murine islets are shown with the low (A) and high (B) concentration analytes separated for ease in viewing. The time that 20 mM glucose was delivered is shown by the bar on top of each plot.

to 680 fmol per islet per min with Ala, Gly, Pro, and Glu having higher secretion rates than other small molecules (Fig. S-3†). Of the 26 small molecules detected from human islets, 25 were also found to be released from murine islets. Similar to the static experiments, the release of Hist was unique to the human islets. The secretion profiles also followed the same trend of decreasing concentration with increasing glucose levels as observed with the murine islet samples. This inverse glucose dependent relationship suggests that the majority of the small molecules may not be released from insulin-containing vesicles, as these would be expected to release during glucose stimulation. It has been suggested that GABA may be released from the cytosol *via* a volume-regulated channel in a pulsatile manner;[35] however, evidence of pulsatile release was not observed in the perfusion experiments here, nor in our previous[13] MEKC experiments.

Overall, secretion rates were found to be higher in human islets compared to murine islets. The differences between both islet species could be due to a variety of variables such as different cellular composition, or the total mass of islets used. Some analytes were not detected when the result from static incubation was compared to that obtained from perfusion experiment. For example, in murine islets, β-ABA, Kyn, TryA, and DA were detected during static incubation but not detected from perfusion experiment. Likewise for human islets, Kyn was the only analyte detected during static incubation that was not detected during perfusion experiments. These subtle differences could be due to the use of different donors, or the levels being too low to detect in the perfused sample. Previous reports using biosensors for ACh have reported its release from human islets;[36] however, we did not detect released ACh in either the

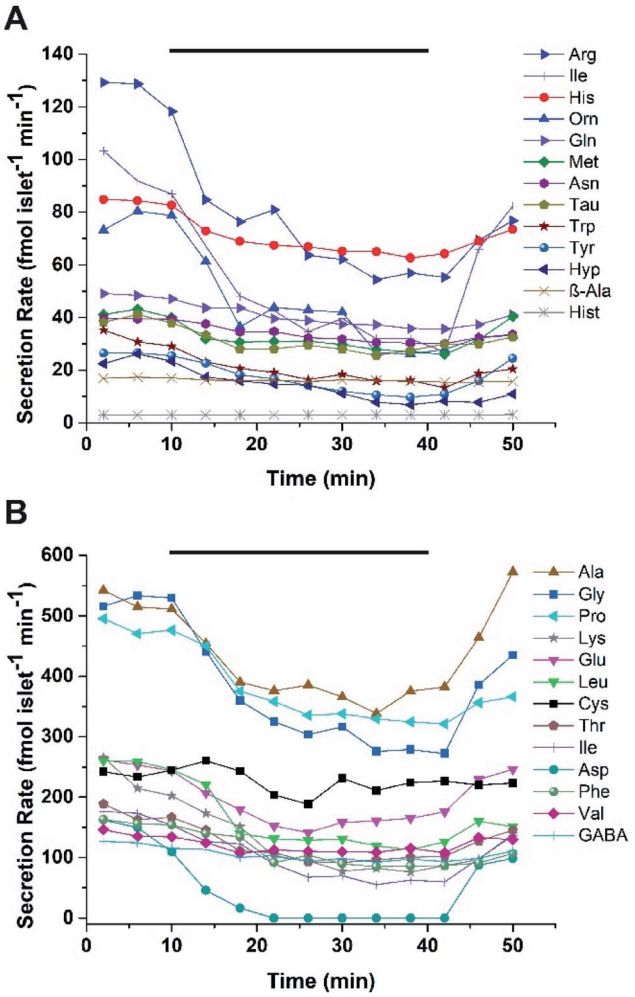

Fig. 4 Secretion profiles of small molecules from human islets. Twenty-five human islets from Donor 2 were perfused using the same protocol as the murine islets. The secretion rates for the low (A) and high (B) concentration analytes are shown. The time that 20 mM glucose was delivered is shown by the bar on top of each plot.

murine or human islets during either the static or perfusion experiments.

4. Conclusions

In this report, an LC-MS/MS method for monitoring small molecule secretions from islets of Langerhans was developed. BzCl was used to impart chromatographic retention and ensure high ESI efficiency. The use of the core–shell RPLC column resulted in high efficiency peaks with a relatively short analysis time. With this method, the secretion of 39 small molecules from murine and human islets were monitored, and the suppressive effect of glucose on the release was observed. A comparison between small molecules secreted from murine and human islets showed differences in their concentrations and secretion rates, with higher secretion rates observed in human islets. While this report shows initial experiments on how islets release small molecules in response to glucose, further experiments and larger numbers of donors are required to better understand the mechanism(s) behind the suppressive effects observed.

Author contributions

Emmanuel O. Ogunkunle: investigation, validation, writing – original draft and editing. Matthew J. Donohue: resources and writing – review and editing. Daniel J. Steyer: resources and writing – review and editing. Damilola I. Adeoye: resources and writing – review and editing. Wesley J. Eaton: resources and writing – review and editing. Michael G. Roper: investigation, resources, funding acquisition, and writing – review and editing.

Conflicts of interest

MGR is an associate editor of the journal, *Analytical Methods*, and has recused himself from any and all editorial responsibilities related to this publication.

Acknowledgements

We would like to thank Dr Xinsong Lin at Florida State University for his help with instrument maintenance, as well as Yao Wang and I-An Wei for their help with murine islet isolation. This research used resources provided by the Mass Spectrometry Laboratory at the FSU Department of Chemistry and Biochemistry (FSU075000MASS). This work was supported in part by grants from the National Institutes of Health, R01 DK080714, and using resources and/or funding provided by the NIDDK-supported Human Islet Research Network (HIRN, RRID: SCR_014393; **https://hirnetwork.org**; UC4 DK116283 to MGR).

References

1 D. D'Alessio, *Diabetes, Obes. Metab.*, 2011, **13**, 126–132.
2 International Diabetes Federation, *Diabetes Atlas*, 2021, ISBN: 978 2 930229 98 0.
3 G. Bruno, C. Runzo, P. Cavallo-Perin, F. Merletti, M. Rivetti, S. Pinach, G. Novelli, M. Trovati, F. Cerutti and G. Pagano, *Diabetes Care*, 2005, **28**, 2613–2619.
4 N. Holman, B. Young and R. Gadsby, *Diabetic Med.*, 2015, **32**, 1119–1120.
5 P. J. Lefèbvre, *Diabetes Care*, 1995, **18**, 715–730.
6 Q. Wang, X. Liang and S. Wang, *Front. Physiol.*, 2013, **3**, 1–8.
7 B. Göke, *Int. J. Clin. Pract.*, 2008, **62**, 2–7.
8 L. S. Satin and T. A. Kinard, *Endocrine*, 1998, **8**, 213–223.
9 R. Rodriguez-Diaz, D. Menegaz and A. Caicedo, *J. Physiol.*, 2014, **592**, 3413–3417.
10 E. Gylfe and A. Tengholm, *Diabetes, Obes. Metab.*, 2014, **16**, 102–110.
11 E. S. Di Cairano, S. Moretti, P. Marciani, V. F. Sacchi, M. Castagna, A. Davalli, F. Folli and C. Perego, *J. Cell. Physiol.*, 2016, **231**, 756–767.
12 X. Wang, L. Yi, C. Guillo and M. G. Roper, *Electrophoresis*, 2015, **36**, 1172–1178.

13 X. Wang, L. Yi and M. G. Roper, *Anal. Chem.*, 2016, **88**, 3369–3375.
14 K. Evans, X. Wang and M. G. Roper, *Anal. Methods*, 2019, **11**, 1276–1283.
15 T. Higashi and S. Ogawa, *J. Chromatogr. A*, 2020, **1634**, 461679.
16 P. Picotti and R. Aebersold, *Nat. Methods*, 2012, **9**, 555–566.
17 N. L. Kuehnbaum and P. Britz-Mckibbin, *Chem. Rev.*, 2013, **113**, 2437–2468.
18 O. S. Barnaby, Y. Benitex, J. L. Cantone, C. A. Mcnaney, T. V. Olah and D. M. Drexler, *Bioanalysis*, 2015, **7**, 2501–2513.
19 T. Huang, M. R. Armbruster, J. B. Coulton and J. L. Edwards, *Anal. Chem.*, 2019, **91**, 109–125.
20 S. Gao, D. M. Wilson, L. E. Edinboro, G. M. McGuire, S. G. P. Williams and H. T. Karnes, *J. Liq. Chromatogr. Relat. Technol.*, 2003, **26**, 3413–3431.
21 P. Song, O. S. Mabrouk, N. D. Hershey and R. T. Kennedy, *Anal. Chem.*, 2012, **84**, 412–419.
22 X. Zheng, A. Kang, C. Dai, Y. Liang, T. Xie, L. Xie, Y. Peng, G. Wang and H. Hao, *Anal. Chem.*, 2012, **84**, 10044–10051.
23 J. M. T. Wong, P. A. Malec, O. S. Mabrouk, J. Ro, M. Dus and R. T. Kennedy, *J. Chromatogr. A*, 2016, **1446**, 78–90.
24 W. H. Lee, T. Ngernsutivorakul, O. S. Mabrouk, J. M. T. Wong, C. E. Dugan, S. S. Pappas, H. J. Yoon and R. T. Kennedy, *Anal. Chem.*, 2016, **88**, 1230–1237.
25 J. P. Grinias, J. M. T. Wong and R. T. Kennedy, *J. Chromatogr. A*, 2016, **1461**, 42–50.
26 A. Mohebi, J. R. Pettibone, A. A. Hamid, J. M. T. Wong, L. T. Vinson, T. Patriarchi, L. Tian, R. T. Kennedy and J. D. Berke, *Nature*, 2019, **570**, 65–70.
27 A. C. Valenta, C. I. D'Amico, C. E. Dugan, J. P. Grinias and R. T. Kennedy, *Analyst*, 2021, **146**, 825.
28 G. Guiochon and F. Gritti, *J. Chromatogr. A*, 2011, **1218**, 1915–1938.
29 A. R. Lomasney, L. Yi and M. G. Roper, *Anal. Chem.*, 2013, **85**, 7919–7925.
30 X. Wang and M. G. Roper, *Anal. Methods*, 2014, **6**, 3019–3024.
31 W. J. Eaton and M. G. Roper, *Anal. Methods*, 2021, **13**, 3614–3619.
32 A. G. Zestos and R. T. Kennedy, *AAPS J.*, 2017, **19**, 1284–1293.
33 A. M. Schrell, N. Mukhitov, L. Yi, X. Wang and M. G. Roper, *Annu. Rev. Anal. Chem.*, 2016, **9**, 249–269.
34 J. Sibbitts, K. A. Sellens, S. Jia, S. A. Klasner and C. T. Culbertson, *Anal. Chem.*, 2018, **90**, 65–85.
35 D. Menegaz, D. W. Hagan, J. Almaça, C. Cianciaruso, R. Rodriguez-Diaz, J. Molina, R. M. Dolan, M. W. Becker, P. C. Schwalie, R. Nano, F. Lebreton, C. Kang, R. Sah, H. Y. Gaisano, P. O. Berggren, S. Baekkeskov, A. Caicedo and E. A. Phelps, *Nat. Metab.*, 2019, **1**, 1110–1126.
36 R. Rodriguez-Diaz, R. Dando, M. C. Jacques-Silva, A. Fachado, J. Molina, M. H. Abdulreda, C. Ricordi, S. D. Roper, P. O. Berggren and A. Caicedo, *Nat. Med.*, 2011, **17**, 888–892.